VOL. 13, NO. 6, MARCH 2018 ISSN 1819-6608
ARPN Journal of Engineering and Applied Sciences

www.arpnjournals.com

INVESTIGATION OF 1D SHEAR WAVE VELOCITY PROFILE USING THE SPATIAL AUTOCORRELATION (SPAC) METHOD: CASE STUDY AT WEST PARK ITB CAMPUS, BANDUNG, INDONESIA

Wahyu Srigutomo, Gunawan Handayani, Arief R. Pribadi and Aryandi M. Nugraha
Physics of Earth and Complex Systems, Faculty of Mathematics and Natural Sciences, Institut Teknologi Bandung, Jl. Ganesa Bandung, Indonesia
E-Mail: wahyu@fi.itb.ac.id

ABSTRACT

Four-station spatial autocorrelation (SPAC) array measurement to record microtremors was conducted in 2012 at West Park of ITB Ganesa Campus, Bandung, Indonesia. The measurement was aimed at revealing the shallow seismic velocity profile beneath the measured site. Autocorrelation and cross correlation calculations among the center station and the tripartite stations were carried out to provide coherence functions from which the SPAC coefficients were obtained. The SPAC coefficients were fitted to a Bessel function of the first kind of order zero yielding a dispersion curve describing relation between the phase velocity and frequency. Least-squares inversion scheme was applied to invert the dispersion curve into seismic parameters (P and S velocities, density and thickness of layers). The inversion resulted in a shallow four-layer stratified model of shear wave velocity. The shear velocity values are 342, 304 and 468 m/s for the first three layers from the surface down to 30 m deep and 1209 m/s for the half space. Based on the NEHRP classification, the *Vs30* value is equal to 366 m/s indicating that the soil profile beneath the measurement site is categorized as very dense soil or soft rock.

Keyword: spatial autocorrelation (SPAC) array, microtremors, SPAC coefficients, dispersion curve, shears wave velocity.

INTRODUCTION

Microtremors are naturally occurring, low amplitude constant vibrations at the earth surface whose displacements are in the order of 10^{-4} - 10^{-2} mm. These vibrations are caused by all human-related daily activity such as machineries in factories, movement of cars on the road and even people walking on the ground as well as natural phenomena such as ocean wave, rain, atmospheric pressure and river flow [24]. Microtremors are basically consisted of body waves and surface waves. However, since their sources are located at the surface, microtremors comprise mainly surface waves and the vertical components of them can be regarded as Rayleigh waves [30]. Bard [6] presented that microtremors are predominantly surface waves (about 70%) in which low frequency tremors below 0.5 Hz are due to oceanic waves, intermediate frequency tremors between 0.5-1 Hz are generated near coast and from the sea, and high frequency tremors above 1 Hz are associated with human activities. Natural vibrations below 1 Hz are usually termed microseisms.

Records of microtremors generally contain information on complex sources, information on the transmission path, and information on the subsurface structure beneath the observation site [24]. Surface waves which mainly constitute the microtremors are dispersive, that is their velocity varies depending on the frequency. Since dispersion is controlled by subsurface structure, in principle we are able to infer subsurface structure once we have the dispersion curve depicting phase velocity vs. frequency at a station. Micrometremor data have been widely used for site effect studies investigating dominant period and amplification pioneered by Kanai *et al*. [13]. In its development, study of microtremors has been focused on utilization of the spectral ratio of horizontal to vertical components of microtremors know as H/V or HVSR method suggested by Nogoshi and Igarashi [23] using Rayleigh-wave ellipticity as a tool for identification of fundamental frequencies and amplification factors of a particular site especially in urban areas. The H/V method was then extensively promoted by Nakamura [20] [21] [22], followed by the development of numerical schemes to invert the HVSR curves into shear velocity v_s profile depicting vertical stratigraphy of the site [11] [4] [5] [3].

Complex mechanism of microtremors generation are viewed as a stochastic process yielding certain characteristics of surface waves both in time and spatial domains [24]. Surface waves are well understood to exhibit dispersion where the velocity of the surface waves depend on the frequency of the waves, and dispersion itself is controlled by the subsurface structure. Based on this comprehension it is possible to reveal the subsurface structure based on the dispersion. Nowadays, methods of surface waves measurement can be grouped into two main categories: first is the frequency-wavenumber spectral method (*f-k* method) and second is the spatial autocorrelation (SPAC) method. Both methods require an array of stations for a particular site, the minimum number of stations is seven for the *f-k* method and four for the SPAC method. The array of stations can be irregular or scattered for the *f-k* method, whereas the array geometry of the SPAC method must have a centered circular shape. The *f-k* method and its processing algorithms were introduced by several authors such as Toksoz and Lacoss [30], Lacoss *et al.* [15] and Capon [8]. The SPAC method was firstly developed by Aki [1] based on the assumption that microtremors are isotropic waves approaching the measurement site from all directions. SPAC method has

been applied for example in estimating earthquake site effects in urban areas like Mexico City [10] [27]; identification of 2D effects and shear-wave velocity profile in valleys [9]; identification of fault and permeable zones in geothermal areas [32]; inferring subsurface structure of volcanoes such as Vesuvius [18] and characterization of SPAC spectra as a function of source distance.

This paper discusses spectral analysis of microtremor data recorded using four-station triangular array of SPAC method and the inversion of the associated dispersion curve into a 1D layered model of vertical shear velocity structure. The least-squares scheme was applied in the inversion yielding a best model within an acceptable misfit between the observed dispersion curve and the theoretical one.

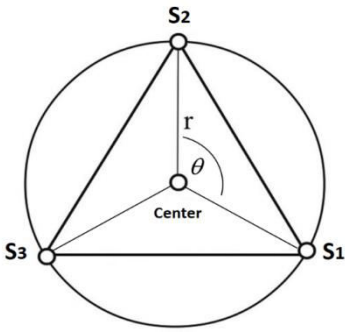

Figure-1. Configuration of four-station array of SPAC method. Center (C), S1, S2 and S3 denote the seismometers and their locations. The distance from Center to all its tripartite stations is *r*.

METHOD

SPAC method

The theoretical basis of SPAC method is originated from a study developed by Aki [1] to understand the relations between the temporal and spatial spectra of microtremors and their phase velocity characteristics. Spectra obtained from field seismic recording can be converted be into phase velocity at certain frequencies. This relationship has become the foundation for the SPAC method dealing with extraction of information from the dispersive Rayleigh waves contained in microtremors. In microtremor records, the recorded waves can be represented by the following equations:

$$u_C = u(0,0,\omega,t) \tag{1}$$

$$u_X = u(r,\theta,\omega,t). \tag{2}$$

Equation (1) represents the wave propagation velocity observed at the center station $C(0, 0)$ whereas Equation (2) represents the wave propagation velocity recorded at the tripartite station $X(r, \theta)$. The illustration of SPAC four-station array is shown in Figure-1.

The SPAC function is the correlation function that measures the covariance at frequency between the microtremors observed at the center C and each tripartite station X [10] [25]:

$$\phi(r,\theta,\omega) = \overline{u(0,0,\omega,t)\cdot u(r,\theta,\omega,t)} \tag{3}$$

where $\overline{u(t)}$ is the average value of velocity in the time domain. From the SPAC function, SPAC coefficient can be derived which is the average of the SPAC function from all directions contained in the circular array,

$$\rho(r,\omega) = \frac{1}{2\pi\cdot\phi(0,\omega)}\int_0^{2\pi}\phi(r,\theta,\omega)d\theta \tag{4}$$

where $\phi(0, \omega)$ is the SPAC function at the center of the array or $C(0, 0)$.

Ideally, all the seismometers in a circular array have the same frequency response which is seldom obtained in a realistic condition. To cope this issue, Equation (4) is expressed as

$$\rho(r,f) = \frac{1}{2\pi}\int_0^{2\pi}\frac{S_{CX}(f,r,\theta)}{\sqrt{S_C(f,0).S_X(f,r,\theta)}}d\theta \tag{5}$$

where $S_{CX}(f, r, \theta)$ is cross spectrum between measured microtremor signal at station X (the tripartite station) and measured signal at the center C. $S_C(f, 0)$ is the power spectral density (PSD) of the measured signal at C. $S_C(f, r, \theta)$ is the PSD of the measured signal at X. $\frac{S_{CX}(f,r,\theta)}{\sqrt{S_C(f,0).S_X(f,r,\theta)}}$ is the coherence function between the measured signals at C and at X. In practice, the SPAC coefficient is calculated by averaging the coherence values of the center and all the tripartite stations.

Dispersion curve

The coefficient of SPAC is related to the seismic phase velocity through the Bessel function of the first kind of order zero [1] [24] [25].

$$\rho(r,f) = J_0\left(\frac{2\pi fr}{c(f)}\right) \tag{6}$$

where $c(f)$ is the phase velocity at frequency f. The curve of SPAC coefficient is fitted to the Bessel equation in order to obtain the argument for the Bessel function (x) which is correlated with the value of $2\pi fr/c(f)$. Therefore for each argument of Bessel function x_i we can find phase velocity at frequency f_i,

$$c(f_i) = 2\pi fr / x_i \ . \quad (7)$$

The procedure of extracting phase velocity from the SPAC analysis basically ends here. The illustration of this procedure is depicted in Figure-2. The obtained dispersion curve represents the values of Rayleigh wave phase velocity beneath the center station. The subsurface structure based on shear-wave velocity distribution is revealed by an inversion scheme to transform the dispersion curve (phase velocity vs. frequency) into profile of shear velocity vs. depth. The inversion scheme requires observed dispersion curve from the field and theoretical curve resulted from forward model calculation.

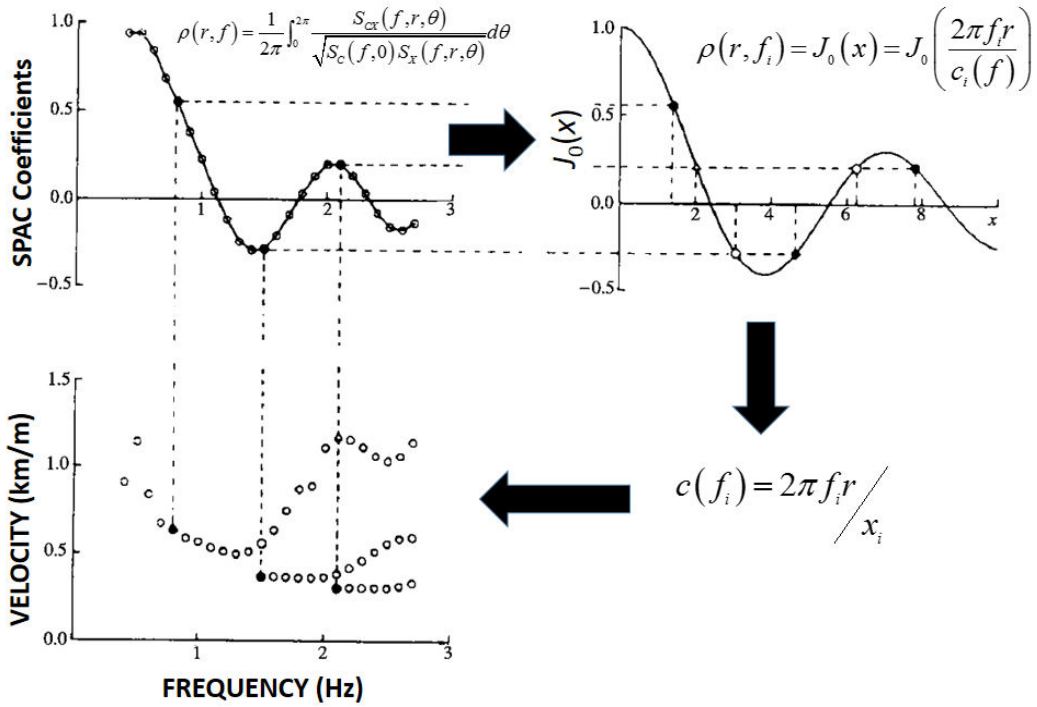

Figure-2. Flowchart for estimating microtremor phase velocity using the SPAC analysis (modified from Okada [24]).

MODELING AND INVERSION

Forward modeling

The phase velocity of Rayleigh wave for a stratified 1D earth can be calculated as a function of wave frequency, medium density, seismic wave propagation velocity in the medium, and thickness of the medium. In a stratified model, each layer is considered to be homogeneous and isotropic. The phase velocity of Rayleigh wave C_{Ri} is determined by an implicit non-linear characteristic equation:

$$F = \left(f_i, C_{Ri}, v_s, v_p, \rho, h\right) = 0, \quad i = 1, 2, ...M \ , \quad (8)$$

where f_i is the linear frequency in Hz, C_{Ri} is the phase velocity of the Rayleigh wave at frequency f_i, v_s = (v_{s1}, v_{s2}, …, v_{sN}) and v_p = (v_{p1}, v_{p2}, …, v_{pN}) are S and P waves velocity vectors respectively with v_{sj} is the S velocity on j-th layer and v_{pj} is the P velocity on the j-th layer. ρ = (ρ_1, ρ_2, …, ρ_j) is the density vector representing density value at each layer, whereas h = (h_1, h_2, …, h_{N-1}) represents thicknesses at each layer. The phase velocity at frequency f_j can be determined from the input parameters (v_s, v_p, ρ, h) as the square root of Equation (8). To obtain all the phase velocities at frequencies f_i (i = 1, 2, …, M), a number of M equations are simultaneously solved in form of Equation (8).

Inverse modeling

In the inversion scheme, the accuracy of partial derivation of phase velocity with respect to the model parameters is the important aspect in modification of model parameters. Low accuracy in determination of partial derivatives may lead to the non-convergence in the inversion scheme [31]. For a 1D stratified earth model, the phase velocity of the Rayleigh wave can be calculated by the Knopoff method [28] using the Taylor expansion on Equation (8) and omitting the second and higher order terms, the residuals between the observed and theoretical data Δc_i can be approximated by first order partial differential equation.

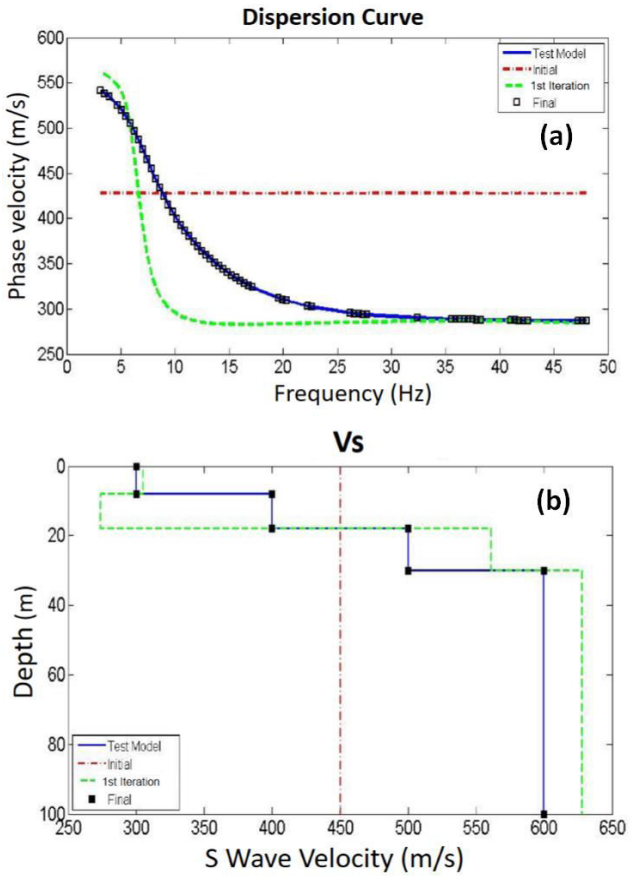

Figure-3. (a) Comparison between the synthetic data generated by the Test Model and the theoretical data. At 5-th iteration the theoretical data converge to the synthetic data giving a minimum misfit. (b) Comparison between the shear-wave velocity v_s of the test model and the inverted model. At the 5-th iteration the inverted model equally converges to the test model.

$$\Delta c_i = \sum_{j=1}^{N}\left(\frac{\partial c_i}{\partial v_{pj}}\Delta v_{pj} + \frac{\partial c_i}{\partial v_{sj}}\Delta v_{sj} + \frac{\partial c_i}{\partial \rho_j}\Delta \rho_j\right) + \sum_{j=1}^{N-1}\left(\frac{\partial c_i}{\partial h_j}\Delta h_j\right), \quad i = 1, 2, \ldots M \tag{9}$$

Partial differentiation can be carried out numerically by Ridder's method [26] or analytically using variational technique and eigen function calculation of the surface wave equation [2]. It is usual to incorporate constraints on the inversion scheme to simplify the calculation, such as making the thicknesses constant and v_p and ρ are regarded as functions of v_s and that the phase velocity is dominated by v_s [24]. The relations between v_p, v_s and ρ have been proposed empirically by several authors (e.g. Hayashi *et al*. [12]; Kitsunezaki *et al*., [14]; Ludwig *et al.* [17]). In this paper, the empirical expression of v_p is taken from Kitsunezaki *et al*. [14],

$$v_p = 1.29 + 1.11 v_s \tag{10}$$

and density is taken from Ludwig *et al*. [17],

$$\rho = 1.2475 + 0.399 v_p + 0.026 {v_p}^2 . \tag{11}$$

v_p and v_s are in km/s whereas ρ is in gr/cm^3. Using the above expressions, Equation (9) can be written in simpler form:

$$\Delta c_i = \sum_{j=1}^{N}\left[\left(\frac{\partial c_i}{\partial v_{pj}}\right)\frac{dv_{pj}}{dv_{sj}} + \left(\frac{\partial c_i}{\partial v_{sj}}\right) + \left(\frac{\partial c_i}{\partial \rho_j}\right)\frac{d\rho_j}{dv_{sj}}\right]\Delta v_{sj}, \quad i = 1, 2, \ldots M \tag{12}$$

where Δv_{sj} becomes the only unknown variable, which suggests that it is only shear-wave velocity structure that can be determined directly from the phase velocity of Rayleigh waves.

There are several assumptions applied in the inversion: 1) the observed phase velocity of microtremors is resulted from the fundamental mode of Rayleigh waves and 2) The structure under the array of observation is parallel or having stratified layers and physical properties in each layer are homogeneous and isotropic. Data to be inverted are the residual of phase velocities as in Equation (12) denoted by an (M x 1) column vector P and the sought parameters are the value of Δv_s in each layer, denoted by an (N x 1) column vector V_s whose relation between both vectors is expressed as:

$$\mathbf{P} = \mathbf{G}\mathbf{V_s}, \tag{13}$$

G is an (M x N) coefficient matrix containing the partial derivatives. The inversion is carried out by the least-squares method, which finds model parameters that minimize residuals expressed by the misfit between the observed and theoretical data.

The least-squares solution is obtained by minimizing the square sum of the residual,

$$\left|\mathbf{e}\right|^2 = \left(\mathbf{P} - \mathbf{G}\mathbf{V_s}\right)^T \left(\mathbf{P} - \mathbf{G}\mathbf{V_s}\right), \tag{14}$$

yielding the estimated solution matrix:

$$\hat{\mathbf{V}}_\mathbf{s} = \left(\mathbf{G}^T\mathbf{G}\right)^{-1}\mathbf{G}^T\mathbf{P}. \tag{15}$$

The solution updates the values of the initial v_s setting up new values of Equation (12) enabling the iteration to be repeated until an acceptable misfit the observed and theoretical data is achieved.

Test of the inversion's performance was carried out by inverting synthetic data in form of dispersion curve generated by a velocity and density structure shown in the Table-1. The generated synthetic data is shown in Figure-

3a. A numerical code developed by Rix and Lai in 2004 (introduced in Lai and Wilmanski [16]) was used to calculate the dispersion curve and the partial derivatives of the phase velocities with respect to the model parameters. The thicknesses are kept fixed and the initial model parameters guessed to initiate the iteration of the inversion are $\rho = 1873$ kg/m^3, $v_p = 1790$ m/s and $v_s = 450$ m/s. At the 5-th iteration, the values of v_s for the test model are fully recovered by the inverted model as shown in Figure 3b, ensuring the validity of the inversion scheme to be used for the analysis of data obtained from the real measurements in the field.

DATA ACQUISITION AND PROCESSING

Location

Microtremor data acquisition for the purpose of this study was carried out at West Park Ganesa Campus of Institut Teknologi Bandung (ITB), Bandung, Indonesia on August 2012. The coordinates of the SPAC array is listed in Table 2 and the surface condition is shown in Figure-4. ITB Campus is situated in an urban area of Bandung City, surrounded by busy streets and commercial activity centers as well as apartments and housing complexes. Previous geotechnical studies in Bandung City indicate that in the northern part of Bandung including the ITB campus, the upper layer is dominated by coarse-grained sand, medium dense to dense, followed by lower layer that is dominated by silty sand to conglomerate and breccia with sandy matrix. Depths of Tertiary base rock vary from 70 to 100 m on west-east direction and from 100 to 120 m on north-south direction [29].

Raw data

Four-station SPAC array with radius of 55 m was placed at the measurement site to record the vertical component of vibrations using four geophones all with a natural frequency of 1 Hz mounted on land-streamer (Figure-4). Each geophone is connected with take-out cables which are also connected to a Seistronix seismograph. The length of the recorded signal is 32 seconds and the sampling rate is 4 ms. The recorded microtremors at all stations are depicted in Figure-5. Microtremors recorded at all stations exhibit almost similar pattern of vibration. Outlier removal was applied to the signals before further processing to remove the unwanted spikes which may not related to the earth's responses. The unwanted spikes tend to concentrate between 0.5 and 1 s and near 3 s.

PSD and SPAC coefficients

Calculation of microtremor PSD from the above mentioned array has resulted four plots of auto spectrum (C-C, S1-S1, S2-S2 and S3-S3) and three plots of cross spectrum (C-S1, C-S2, and C-S3). For examples, Figure 6a depicts the auto spectrum of C-C whereas Figure-6b shows the auto spectrum of S1-S1. The cross spectrum of C-S1 is shown in Figure 6c. The plot of coherence function between the C and S1 is shown in Figure-3d. Basically it indicates the degree of relation between signals recorded at C and at S1. The SPAC coefficient plot as function of frequency is obtained by averaging the three coherence plots. The coherence coefficients are shown in Figure-6e.

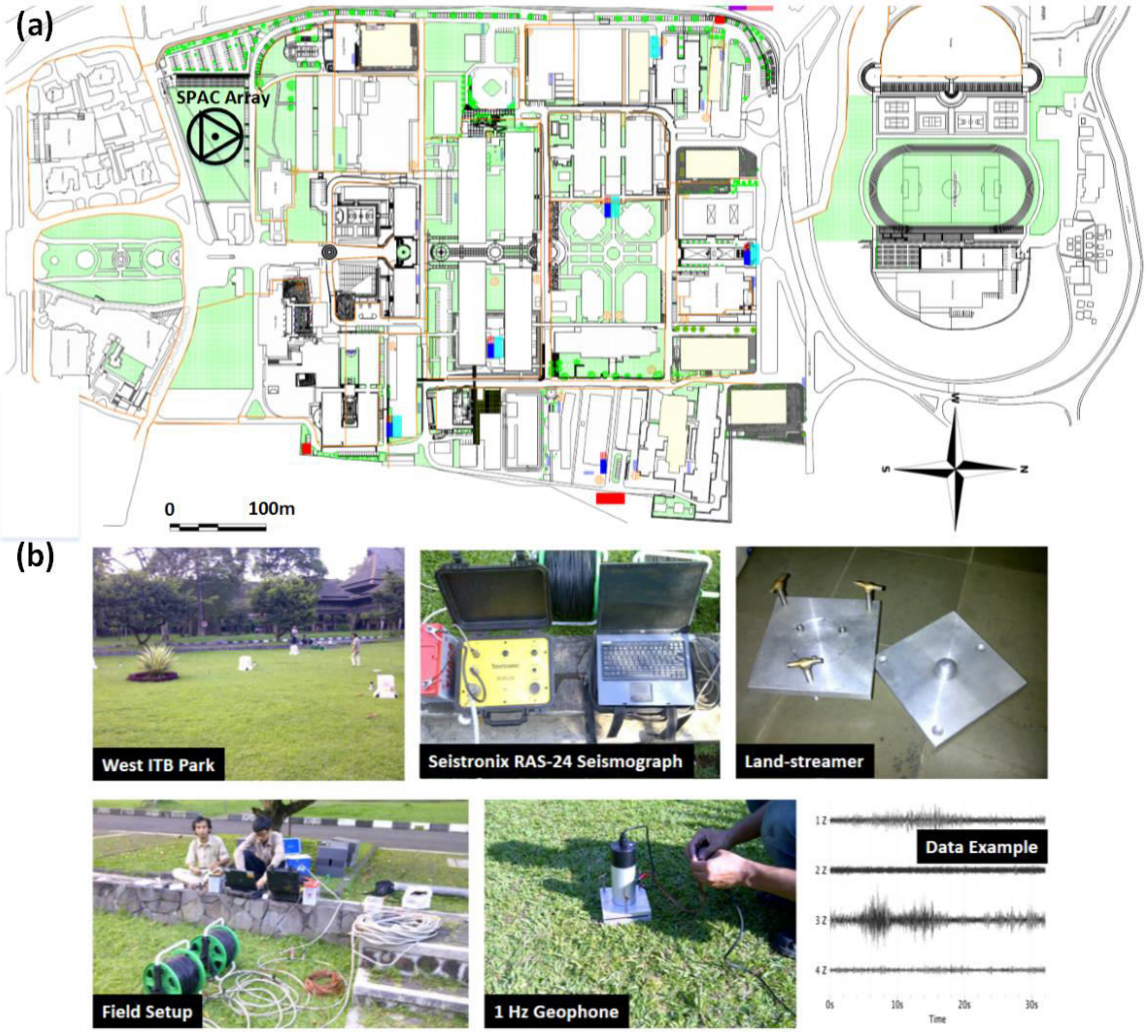

Figure-4. (a) Map of ITB Campus where the SPAC array was deployed at coordinates shown in Table-1. (b) Photographs of the field setup and instruments used during the measurement of microtremors.

Table-1. Parameters of test model for the inversion.

Layer	**Thickness** (m)	ρ (kg/m^3)	v_p (m/s)	v_s (m/s)
1	8	1822	1623	300
2	10	1856	1734	400
3	12	1890	1845	500
half space	infinite	1923	1956	600

Table-2. Coordinate of the four-station array for SPAC measurement.

Station	**Latitude** (°)	**Longitude** (°)	**Easting - UTM** (m)	**Northing - UTM** (m)
C	6.89285 S	107.60934 E	788367.001	9237307.710
S1	6.89310 S	107.60977 E	788414.402	9237279.786
S2	6.89234 S	107.60934 E	788367.310	9237364.146
S3	6.89310 S	107.60890 E	788318.191	9237280.312

Table-3. Inverted model parameters based on micritremors recorded by SPAC array at ITB West Park.

Layer	**Thickness** (m)	ρ (kg/m^3)	v_p (m/s)	v_s (m/s)
1	8	1836	1670	342
2	10	1823	1627	304
3	12	1879	1809	468
half space	infinite	2113	2632	1209

Table-4. Typical rock velocities and density [19].

Type of formation	**P wave velocity** (m/s)	**S wave velocity** (m/s)	**Density** (g/cm^3)	**Density of constituent crystal** (g/cm^3)
Scree, vegetal soil	300-700	100-300	1.7-2.4	-
Dry sands	400-1200	100-500	1.5-1.7	2.65 quartz
Wet sands	1500-2000	400-600	1.9-2.1	2.65 quartz
Saturated shales and clays	1100-2500	200-800	2.0-2.4	-
Marls	2000-3000	750-1500	2.1-2.6	-
Saturated shales and sand sections	1500-2200	500-750	2.1-2.4	-
Porous and saturated sandstones	2000-3500	800-1800	2.1-2.4	2.65 quartz
Limestones	3500-6000	2000-3300	2.4-2.7	2.71 calcite
Chalk	2300-2600	1100-1300	1.8-3.1	2.71 calcite
Salt	4500-5500	2500-3100	2.1-2.3	2.1 halite
Anhydrite	4000-5500	2200-3100	2.9-3.0	-
Dolomite	3500-6500	1900-3600	2.5-2.9	(Ca,Mg) CO_3 2.8-2.9
Granite	4500-6000	2500-3300	2.5-2.7	-
Basalt	5000-6000	2800-3400	2.7-3.1	-
Gneiss	4400-5200	2700-3200	2.5-2.7	-
Coal	2200-2700	1000-1400	1.3-1.8	-
Water	1450-1500	-	1.0	-
Ice	3400-3800	1700-1900	0.9	-
Oil	1200-1250	-	0.6-0.9	-

RESULTS AND DISCUSSIONS

Dispersion curve

The dispersion curve was obtained by fitting the SPAC coefficients with the values of Bessel function of the first kind of order zero. In this work, fitting was carried out if the misfit is below 10^{-4}, resulting an array of data containing frequencies and Bessel arguments. These variables were used to calculate the phase velocity as a function of frequency or dispersion curve using Equation 7 as shown in Figure-7. At the lowest frequency the phase velocity is about 1050 m/s, whereas at about 48 Hz the phase velocity is about 375 m/s, and the slowest phase velocity is about 225 m/s at 16 Hz. This feature indicates that the shear velocity structure is not consistently increasing towards depths. Instead, the smallest shear-wave velocity lays in a layer between the first layer and the deeper half space.

Inverted shear-wave velocity model

The inversion scheme is intended to transform the dispersion curve (phase velocity vs. frequency) into velocity structure (shear wave velocity vs. depth) using the least-squares method. There are 4 layers (n = 4) of shear velocity involved in the inversion: the first three layers whose thicknesses are variable overlying a homogeneous half space. The total number of sought model parameters is $4n$ - 1 or 15 in this case (3 parameters of h, 4 parameters of v_s, 4 parameters of v_p and 4 parameters of ρ). The initial model is a homogeneous structure having v_s = 450 m/s. At the first iteration the root mean square (rms) misfit is 32% and the minimum rms misfit of 4% is achieved at 17-th iteration before bouncing up and down between rms

misfits of 4 - 5% up to 26-th iteration. The comparison between the observed dispersion curve and the theoretical one and the inverted model shear velocity layers at 17-th iteration are shown in Figure-8. The overall inverted model parameters are listed in Table-3. It is confirmed by the inverted parameters that the lowest value of velocity layer lays between two higher velocity layers as suggested by the observed dispersion curve. Density and seismic velocities can be used to estimate the types of subsurface materials. Values of these physical parameters for several types of rocks are listed in Table-3.

Based on the inverted seismic parameters and those listed in Table-4, the first two layers may be attributed to dry sand, the third layer may represent saturated shales and sand sections, followed by saturated sandstone representing the half space. The presence of dry sand and saturated sandstone indicates that the area of measurement is situated on a recharge area.

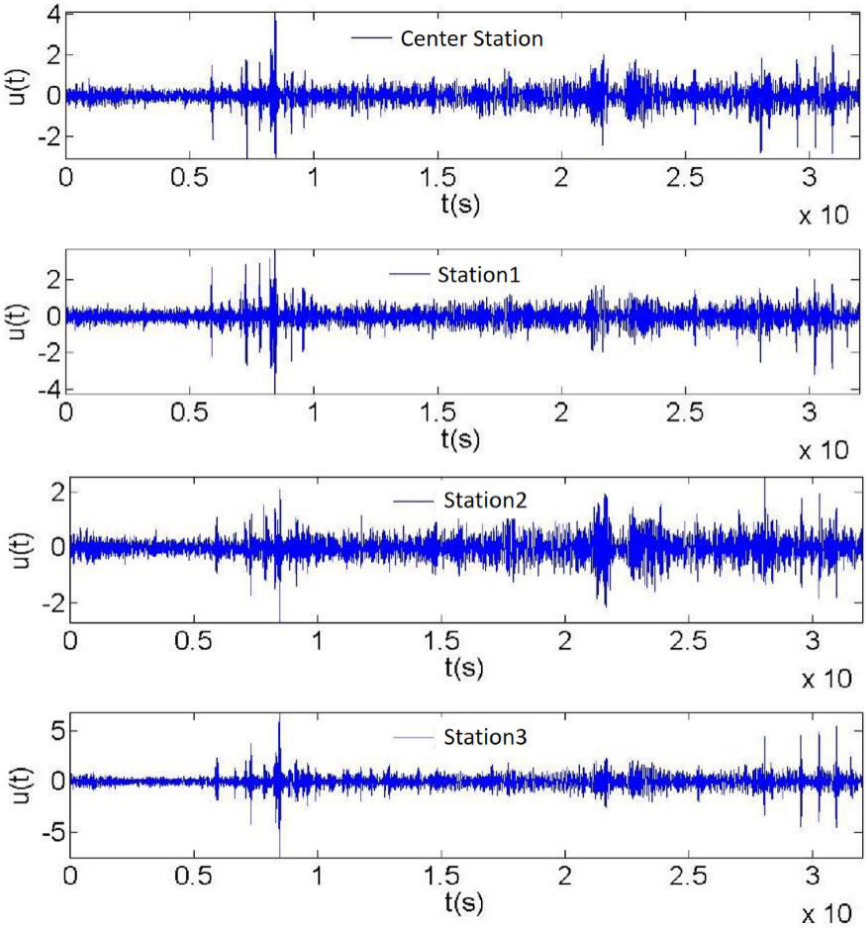

Figure-5. Raw microtremor signals recorded at stations C, S1, S2, and S3 on ITB Campus, Bandung, Indonesia.

Besides the information of types of subsurface materials, information of soil profile is also important from geotechnical point of view, which emphasizes the soil characteristics down to 30 m deep in term of shear velocity which is called *Vs30*. Soil profile is intended to classify the strength level of soil associated with risk of ground shaking to buildings built on it. Soft soil (low shear velicity) amplifies ground shaking caused by earthquake. The National Earthquake Hazards Reduction Program (NEHRP) classify soils into six types based on their *Vs30* [7]: (A) hard rock > 1500 m/s; (B) rock 760 - 1500 m/s; (C) very dense soil/ soft rock 360 - 760 m/s; (D) stiff soil 180 - 360 m/s; (E) soft soil < 180 m/s; and (F) special soil, requiring site specific evaluation. *Vs30* calculation was carried out using the following formula:

$$Vs_{30} = \frac{\sum_{i=1}^{n} d_i}{\sum_{i=1}^{n} \frac{d_i}{vs_i}}, \quad (16)$$

yielding a value of 366 m/s which falls into category of very dense soil or soft rock but close enough to stiff soil profile. This type of soil is usually consisted of granular grains including gravel, sand and loamy sand or soil where water is freely seeping consistent with that is described by Sengara *et al*. [29] previously or submerged rock which is regarded unstable. The study area is located between the zones of maximum amplification factor (1.65) in the southern part of Bandung City and of minimum amplification factor (1.35) in the northern part [29].

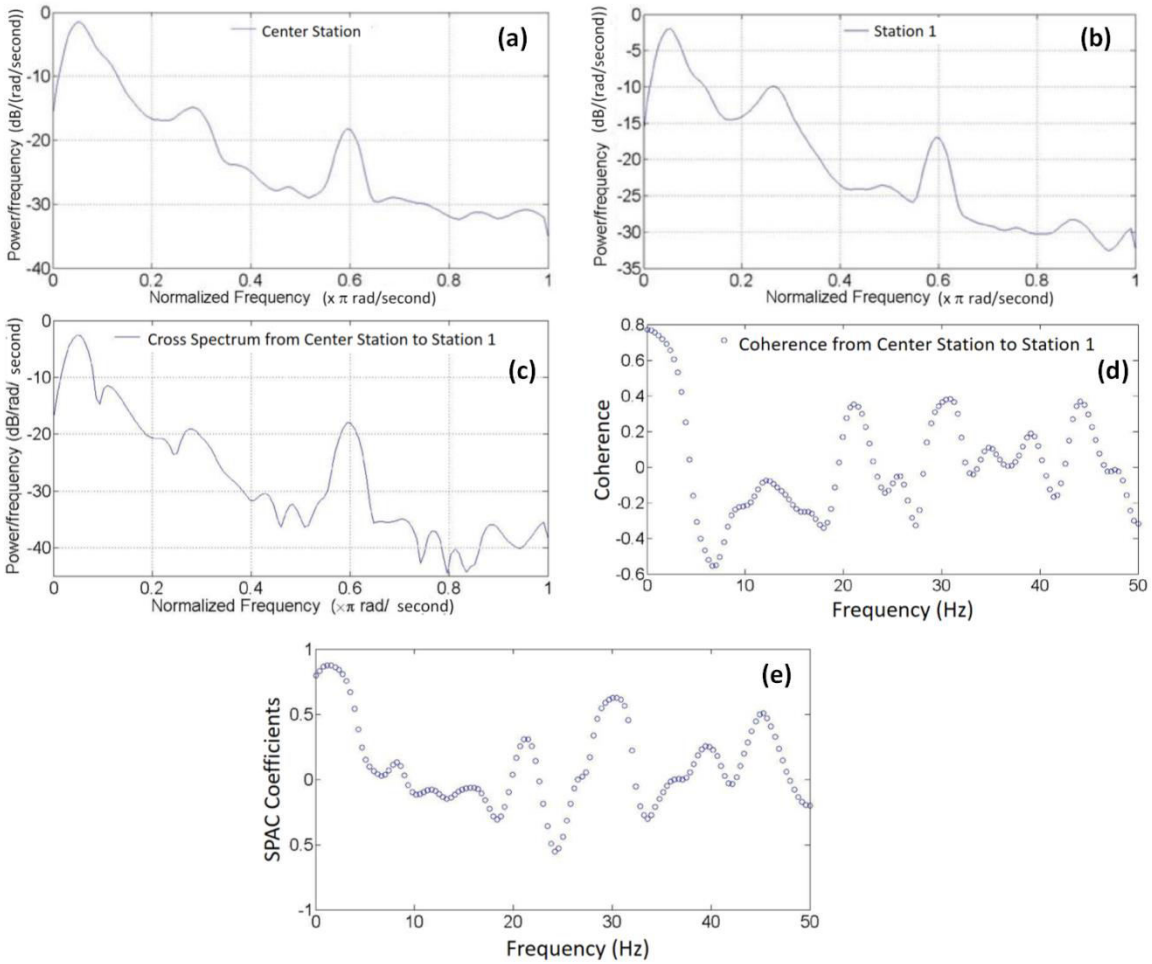

Figure-6. (a) Auto spectrum of C-C. (b) Auto spectrum of S1-S1. (c) Cross spectrum of C-S1. (d) Coherence function between C and S1. (e) SPAC coefficients obtained from averaging the coherence plots.

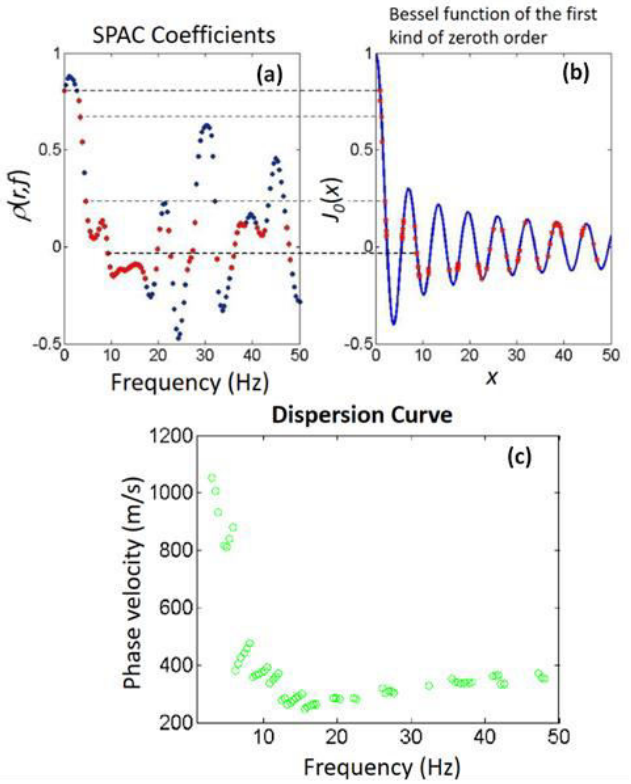

Figure-7. Fitting of the SPAC coefficients with the Bessel function of the first kind of order zero to produce the dispersion curve of the measurement array.

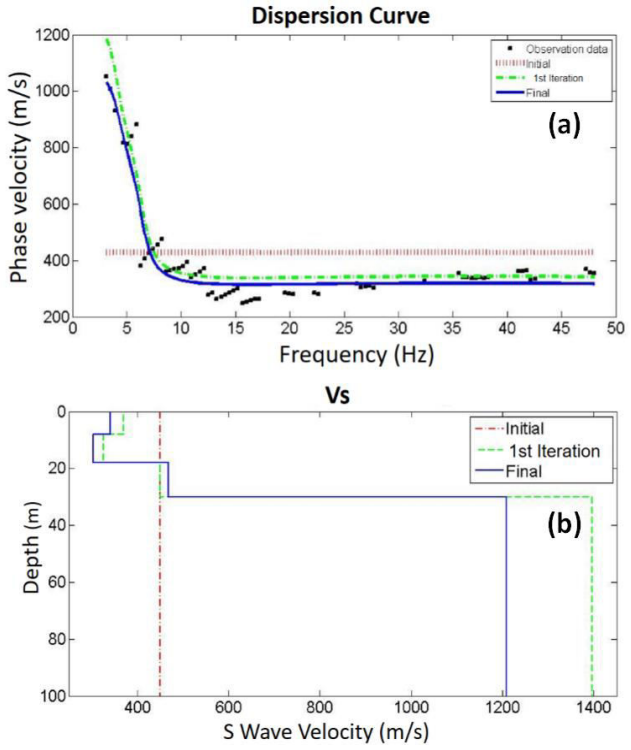

Figure-8. (a) The comparison between the observed and the calculated dispersion curve of microtremors recorded at ITB West Park, Bandung, Indonesia. (b) The inverted v_s structure obtained from inversion of the observed dispersion curve.

CONCLUSIONS

Microtremor data acquisition for for-station SPAC array has been conducted at the West Park ITB Ganesa Campus, in Bandung, Indonesia. The recorded signals was processed to provide SPAC coefficients from which by fitting with the Bessel function of the first kind of order zero the dispersion curve was obtained. The dispersion curve in inverted by the least-squares method to reveal a shallow four-layer stratified model of shear wave velocity. The velocity values are 342, 304 and 468 m/s for the first three layers from the surface down to 30 m deep and 1209 m/s for the half space. Based on the NEHRP classification, the *Vs30* value is equal to 366 m/s indicating that the soil profile beneath the measurement site is categorized as very dense soil or soft rock.

ACKNOWLEDGEMENTS

The authors wish to thank the members of Earth Physics Laboratory, Faculty of Mathematics and Natural Sciences, Institut Teknologi Bandung for their support during the preparation and field data acquisition steps.

REFERENCES

[1] Aki K. 1957. Space and time spectra of stationary stochastic waves, with special reference to microtremors, Bull. Earthq. Res. Inst. 35, pp. 415-456.

[2] Aki K. and Richards P. G. 1980. Quantitative seismology: W.H. Freeman & Co.

[3] Albarello, D. and Lunedei, E., 2009. Alternative interpretations of horizontal to vertical spectral ratios of ambient vibrations. New insights from theoretical modelling, Bulletin of Earthquake Engineering, vol. 8, no. 3, pp. 519 - 534.

[4] Arai H. and Tokimatsu K. 2004. S-Wave velocity profiling by inversion of microtremor H/V spectrum, Bulletin of the Seismological Society of America. 94(1): 53-63, doi: 10.1785/0120030028.

[5] Arai H. and Tokimatsu K. 2005. S-wave velocity profiling by joint inversion of microtremor dispersion curve and horizontal-to-vertical (H/V) spectrum, Bulletin of the Seismological Society of America. 95(5): 1766-1778, doi: 10.1785/0120040243.

[6] Bard P. 1998. Microtremor Measurements: A tool for site effect estimation? The effects of Surface Geology on Seismic Motion, Proceeding of The Second International Symposium on the Effects of Surface Geology on Seismic Motion, Yokohama, Japan. 3, 1251-1279.

[7] Building Seismic Safety Council (BSSC). 1997. NEHRP, recommended provisions for seismic regulations for new buildings, Part 1-Provisions (FEMA Federal emergency Management Agency. 302): 290.

[8] Capon J. 1969: High-resolution frequency-wavenumber spectrum analysis, Proc. IEEE 57, no. 8, pp. 1408-1418, doi:10.1109/PROC.1969.7278

[9] Claprood M., Asten M.W. and Kristek J. 2011. Using the SPAC Microtremor Method to Identify 2D Effects and Evaluate 1D Shear-Wave Velocity Profile in Valleys, Bulletin of the Seismological Society of America. 101(2): 826-847, doi: 10.1785/0120090232.

[10] Estrella H. F. and González J. A. 2003: SPAC: An alternative method to estimate earthquake site effects in Mexico City, Geofísica Internacional. 42 (2): 227-236.

[11] Fah D., Kind F. and Giardini D. 2003. Inversion of local S-wave velocity structures from average H/V ratios, and their use for the estimation of site-effects, Journal of Seismology. 7: 449-467.

[12] Hayashi K., Inazaki K. and Suzuki H. 2005. Buried Channel Delineation using Microtremor Array Measurements. SEG Technical Program Expanded Abstracts, pp. 1137-1140, doi: 10.1190/1.2147882.

[13] Kanai K., Osada T. and Tanaka T. 1954. An investigation into the nature of microtremors. Bull. Earthq. Res. Inst. 32, 199-209.

[14] Kitsunezaki C., Goto N., Kobayashi Y., Ikawa T., Horike M., Saito T., Kurota T., Yamane K. and Okuzumi K. 1990. Estimation of P- and S- wave velocities in deep soil deposits for evaluating ground vibrations in earthquake: SizenSaigai-Kagaku. 9, pp. 1-7.

[15] Lacoss R., E. Kelly and Toksöz M. 1969. Estimation of seismic noise structure using arrays, Geophysics. 34(1): 21-38, doi: 10.1190/1.1439995.

[16] Lai, C. G. and Wilmanski, K. (eds). 2005. Surface Waves in Geomechanics: Direct and Inverse Modelling for Soils and Rocks, Springer, Wien - New York.

[17] Ludwig W. J., Nafe J.E. and Drake C.L. 1970. Seismic refraction in the sea, part 1: Wiley-Interscience. 74.

[18] Maresca R., Nardone L., Galluzzo D., La Rocca M. and Del Pezzo E. 2006. Application of the SPAC Method to Ambient Noise Recorded in the Vesuvius Area (Italy), Third International Symposium on the Effects of Surface Geology on Seismic Motion, Grenoble, France, 30 August - 1 September 2006 Paper Number: 073 pp. 1-6.

[19] Mavko G. 2016. (n.d.). Conceptual Overview of Rock and Fluid Factors that Impact Seismic Velocity and Impedance Stanford Rock Physics Laboratory, pp. 73-112, https://pangea.stanford.edu/courses/gp262/Notes/8.SeismicVelocity.pdf (accessed on 20 July 2016).

[20] Nakamura Y. 1989. A method for dynamic characteristics estimation of sub-surface using microtremor on the ground surface, Quarterly Report of Railway Technical Research Institute (RTRI) Vol. 30, No. 1, 25-33.

[21] Nakamura Y. 1996: Real-time information systems for hazards mitigation, Proceedings of the 11th World Conference on Earthquake Engineering, Acapulco, Mexico.

[22] Nakamura Y. 2000. Clear identification of fundamental idea of Nakamura's technique and its applications. Proceeding of the 12th World Conference on Earthquake Engineering, Auckland, New Zealand.

[23] Nogoshi M. and Igarashi T. 1971. On the amplitude characteristics of microtremor (part2), Journal of Seismological Society of Japan 24, 26-40 (In Japanese with English abstract).

[24] Okada H. 2003. The Microtremor Survey Method (translated by Koya Suto): Geophysical Monograph Series, No.12, Society of Exploration Geophysicists.

[25] Okada H. 2006. Theory of efficient array observations of microtremors with special reference to the SPAC method, Exploration Geophysics. 37, pp. 73-85, doi: 10.1071/EG06073.

[26] Press W.H., Teukolsky S.A., Vetterling W.T. and Flannery B.P. 1992. Numerical Recipes in C: The art of scientific computing, 2ed. Cambridge University Press.

[27] Roberts J. and Asten M. 2006. Investigation of near source effects in array-based (SPAC) microtremor survey Earthquake Engineering in Australia. Canberra 24-26 November. pp. 251-256.

[28] Schwab F. A. and Knopoff L. 1972. Fast surface wave and free mode computations: Methods in Computational Physics, 11, Academic Press Inc.

[29] Sengara I. W., Munaf Y., Aswandi A. and Susila I.G.M. 2001. Seismic Risk and Site Response Analysis for City of Bandung-Indonesia. Fourth International Conference on Recent Advances in Geotechnical Earthquake Engineering and Soil Dynamics, 26-31 March, paper 8.

[30] Toksoz M.N. and Lacoss R.T. 1968. Microtremors-mode structure and sources, Science. 159, 872-873.

[31] Xia J., Miller R.D., Park C.B. 1999. Estimation of near-surface shear-wave velocity by inversion of Rayleigh waves, Geophysics, 64, pp. 691-700, doi: 10.1190/1.1444578

[32] Xu P., Ling S., Li C., Du J., Zhang D., Xu X., Dai K. and Zhang Z. 2012. Mapping deeply-buried geothermal faults using microtremor array analysis, Geophys. J. Int. 188, pp. 115-122 doi: 10.1111/j.1365-246X.2011.05266.x.